Phase Noise of Optical Pulse Trains Generated by Talbot Effect in Frequency Shifting Loops

Vincent Billault, Vincent Crozatier, Ghaya Baili, Loic Morvan, Daniel Dolfi, Nithyanadan Kanagaraj, Hugues Guillet de Chatellus

Phase Noise of Optical Pulse Trains Generated by Talbot Effect in Frequency Shifting Loops

Vincent Billault, Vincent Crozatier, Ghaya Baili, Loïc Morvan, Daniel Dolfi, *Fellow, OSA,* Nithyanadan Kanagaraj, *Member, OSA,* and Hugues Guillet de Chatellus

***Abstract*—High repetition rate optical pulse trains are essential for a wide range of applications, including photonic-assisted sampling. Among the different solutions proposed so far, Talbot lasers, based on the generation of an optical frequency comb in a frequency shifting loop, are a simple yet efficient source of short transform-limited pulses. By controlling the comb spectral phase, the repetition rate is reconfigurable. It can be set to a (possibly large) multiple of the comb spacing and reach the GHz range, while only requiring a low bandwidth synthesizer (typ. 100 MHz). The noise characteristics of this pulse trains is a key factor for its application. Therefore, we investigate the phase noise properties of Talbot lasers. In particular, we prove theoretically and demonstrate experimentally that the phase noise at high offset frequency from the carrier, does not depend on the multiplication factor q. We also demonstrate that the phase noise at low offset frequencies, which increases as $20\log q$, can be strongly reduced by a simple locking technique. Finally, we show that in addition to their reconfigurability, Talbot lasers can provide timing jitters at 8.2 GHz as low as 350 fs (integrated from 10^5 Hz to the Nyquist frequency), making them suitable candidates for time metrology applications.**

I. Introduction

The growing need for real-time processing of broadband analog signals is driven by numerous applications, ranging from radar and telecommunications to intelligence systems, especially for highly demanding security applications. To meet these challenges, the performance of analog-to-digital converters (ADCs) is a critical issue [1]. Recall that analog-to-digital conversion consists of time sampling followed by signal quantization. The performance of the ADC is directly set by the purity of the clock signal: any time jitter of the sampling clock will result in erroneous values of the digitized signal. If the clock jitter is assumed to be the only noise source of the ADC unit, then one can define the sampler SNR as: $\mathrm{SNR} = -20\log(2\pi\sigma_J \mathrm{BW})$, where σ_J is the clock jitter integrated up to the Nyquist frequency and BW is the analog bandwidth of the input signal [2]. Therefore, considering an ideal quantization device, the fidelity of the overall analog-to-digital conversion (defined by the effective number of bits, ENOB) is directly set by the sampler SNR, i.e., by the clock jitter. As the instantaneous bandwidth gets larger, the jitter requirement gets stronger to keep the ENOB constant [3]. For several years, electronic solutions have struggled to overcome the 100 fs jitter barrier [4], limiting the potential BW to 3 GHz for an ENOB of 8, or equivalently the ENOB to 6.5 for a 10 GHz BW. Until now, only photonic-assisted solutions have been able to produce multi GHz clock signals, with temporal jitter lower than a hundred of fs. Different architectures for RF signals ADC involving photonics have been proposed over the last twenty years [5], all based on mode-locked (ML) lasers [6]. The latter generate combs of mutually phase-locked optical frequencies, whose spacing (or free spectral range, FSR) is set by the length of the cavity. In the temporal domain, this corresponds to pulses at a repetition rate equal to the cavity free spectral range. However, reaching multi-GHz repetition rates in ML lasers requires specific technologies. In conventional passive ML lasers, in spite of remarkable purity of the pulse train [7], the repetition rate is set by the length of the laser cavity, rendering it challenging to go beyond the GHz range [8]. A first approach to multiply the repetition rate is based on spectral filtering, where the ML frequency comb is filtered by a Fabry-Perot cavity [9], [10]. Only comb lines matching the resonance condition of the Fabry-Perot are transmitted, resulting in a multiplication of the repetition rate, but at the price of a significant decrease of the output power and imperfect rejection of the unwanted lines. A different technique that preserves the output average power, makes use of pulse interleaving [11]. But none of these approaches enables simple tunability of the repetition rate. To circumvent this limitation, active harmonic mode-locking (HML) has been proposed, where multiple short pulses circulate in the laser cavity, enabling the multiplication of the repetition rate of the laser up to several tens of GHz [12], [13]. HML is achieved by modulating the intracavity light at a frequency equal to a large multiple of the cavity FSR. HML offers both reconfigurability of the repetition rate and low timing jitter. However, this technique utilizes an RF signal at the same frequency as the pulse train. Additionally, it has been shown that at low offset frequency from the carrier, the phase noise of the pulse trains follows the one of the RF synthesizer [13], which sets a strong requirement on the spectral purity of the synthesizer. Moreover, the spectral purity of the pulse train is degraded by supermode fluctuations [14], an effect that can be minimized by inserting a resonator in the laser cavity, again to the detriment of tunability [15].

An attractive approach to multiply the repetition rate of a ML pulse train without involving a multi-GHz RF signal source, is to make use of the temporal Talbot effect [16], [17]. A ML pulse train traveling through a transparent medium exhibiting group velocity dispersion, acquires a quadratic spec-

V. Billault, N. Kanagaraj, and H. Guillet de Chatellus are with the LIPhy, UGA/CNRS, 38000 Grenoble, France. e-mail: hugues.guilletdechatellus@univ-grenoble-alpes.fr.

V. Billault, V. Crozatier, G. Baili, L. Morvan, and D. Dolfi are with Thales Research and Technology France, 91767 Palaiseau, France.

Manuscript received May XX, 2020; revised May XX, 2020.

tral phase. Provided the total group-delay dispersion (slope of the linear group delay as a function of radial frequency) experienced by the pulse trains matches $D_2 = \frac{1}{2\pi}\frac{p}{q}T^2$, where T is the laser repetition rate, p and q are mutually prime integers, the repetition rate of the pulse train at the output of the dispersive line is multiplied by q (i.e. is equal to q/T), a phenomenon called temporal fractional Talbot effect [17], [18]. Since Talbot effect is a pure phase modulation process in the spectral domain, the laser power is conserved. Regarding the purity of the pulse train, it has been shown that in the case of input pulses with fluctuating times of arrival, Talbot effect shows an intrinsic improvement of the pulses regularity, in both integer and fractional conditions [19], [20], [21], [22], [23], [24]. However, an important technical limitation of pulse multiplication by temporal Talbot effect is the lack of highly dispersive transparent media. For example, multiplying by a factor of 25 the repetition rate of a 10 GHz ML laser at 1550 nm would require the use of 20 km of single mode fiber (SMF 28). The same multiplication factor for a 100 MHz-repetition rate ML laser, would imply an unrealistic fiber length of 200000 km. Therefore, in practice, Talbot effect can be applied to pulse trains with multi-GHz repetition rates. Moreover, the tunability of conventional temporal Talbot effect is very limited, since a given propagation length is associated to a definite multiplication factor. Notice that several techniques can be used to allow tunability of the repetition rate, but at the expense of significant additional complexity of the system [25], [26].

Recently, a new concept of laser sources with a tunable repetition rate, also based on the temporal Talbot effect, has been demonstrated [27], [28]. In this architecture termed as Talbot laser and based on a frequency shifting loop (FSL), a comb of optical frequencies is created by repetitive passes of a monochromatic CW laser (frequency: f_0), in a loop containing a frequency shifter. The frequencies of the comb teeth (labeled by n) are equal to $f_0 + nf_s$, where f_s is the frequency shift per roundtrip [29]. It can be shown that the spectral phase is quadratic: the phase of the comb tooth n is equal to $\pi f_s \tau_c n^2$, where τ_c is the roundtrip time of the light in the loop [30]. In this system, contrary to conventional temporal Talbot effect, the quadratic spectral phase is not set by the propagation in a dispersive medium, but is directly created by the recirculation of the CW laser in the FSL, i.e. a device combining a spectral with a temporal delay. A Talbot laser can be seen as the equivalent of a ML laser after propagation through a total group-delay dispersion equal to $D_2 = \frac{1}{2\pi}\frac{\tau_c}{f_s}$, which can be controlled by adjusting the system's parameters, f_s and τ_c. Multiplication factors as large as a few hundreds have already been reported, demonstrating the capability of these systems as a simple source of short pulses with a reconfigurable repetition rate [30]. Moreover, compared to HML lasers, Talbot lasers only require a low frequency RF synthesizer (typ. 100 MHz). Therefore Talbot lasers are ultimately an attractive solution for the generation of ps pulses trains with reconfigurable multi-GHz repetition rates. However the spectral purity of this architecture has not been investigated so far.

The objective of this article is to address the question of the phase noise of Talbot lasers. In the second section, we consider a generic comb of optical frequencies (FSR: f_s), whose individual lines are subjected to phase fluctuations. In this specific frame, we express the resulting intensity as a sum of beatnotes, of frequencies qf_s. This enables us to provide an expression of the phase noise of the pulse train of a ML laser ($q = 1$), and of a ML laser with fractional temporal Talbot effect ($q > 1$). In the third part, we address the specific case of the Talbot laser, where the phase fluctuations of the optical comb lines are not independent, but are related to each other by the generation process of the comb in the FSL. More specifically, we obtain a set of two transfer functions, that relate the phase noise spectral density of the pulse train (i.e. of the beatnote at frequency qf_s), with the power spectral densities of two different sources of phase fluctuations: one in the injection arm, and the other one in the FSL itself. Moreover, we show that, at small offset frequencies from the carrier, the phase noise increases as $20\log q$. On the contrary, at high offset frequencies, the phase noise does not depend on q, a result that differs substantially from the analog frequency multiplication process. In the fourth section, we provide an experimental characterization of the phase noise in a Talbot laser, and evidence the agreement of the experimental data with the theory. In the fifth part, we propose a simple solution to strongly reduce the phase noise at low frequency, by implementing a feedback loop. Finally, in the conclusion section, we discuss the limitations of our approach, and provide some perspectives of Talbot lasers.

II. Phase noise of an optical frequency comb with phase fluctuations

In this section, we define the general framework of our study. We consider an optical frequency comb starting at f_0 with a free spectral range of f_s (Fig. 1). We assume that each individual comb line (frequency: f_0+nf_s) experiences a phase fluctuation characterized by the function $\phi_n(t)$. The complex electric field writes:

$$E(t) = \sum_{n=0}^{N} E_n e^{i2\pi(f_0+nf_s t)} e^{i\phi_n(t)}, \tag{1}$$

where E_n are the complex amplitudes of the comb lines. The intensity, defined as $I(t) = E(t)E^*(t)$, is given by:

$$I(t) = \sum_{n,m=0}^{N} E_n E_m^* e^{i2\pi(n-m)f_s t} e^{i(\phi_n(t)-\phi_m(t))}. \tag{2}$$

The intensity consists of the addition of beatnotes, the frequencies of which are multiples of f_s. More specifically, for any value of q, the beatnote at frequency qf_s writes: $I_q(t) = 2\Re(\tilde{I}_q(t)e^{i2\pi q f_s t})$. $\tilde{I}_q(t)$, the slowly varying envelope of the beatnote $I_q(t)$, is equal to:

$$\tilde{I}_q(t) = \sum_{n=q}^{N} E_n E_{n-q}^* e^{i(\phi_n(t)-\phi_{n-q}(t))}. \tag{3}$$

At this point, it is noteworthy that a constant phase in the terms E_n would cancel in Eq. 3. Moreover, one can also notice that, if the complex amplitude terms E_n have a phase term

that evolves linearly with n, this only results in a phase shift of the beatnote at qf_s, but it does not affect its phase noise. We assume in the following that the phase fluctuations of the individual lines $\phi_n(t)$ are much smaller than 2π. Then,

$$\tilde{I}_q(t) = \sum_{n=q}^{N} E_n E_{n-q}^{*}\Big(1 + i(\phi_n(t) - \phi_{n-q}(t))\Big). \quad (4)$$

The phase of the beatnote at frequency qf_s is simply given by: $\psi_q(t) = \arg(\tilde{I}_q(t))$, and is directly set by the complex amplitude of the comb lines E_n.

In the following, we discuss two common cases: the case of a ML frequency comb, and the case of a ML frequency comb in a temporal Talbot condition.

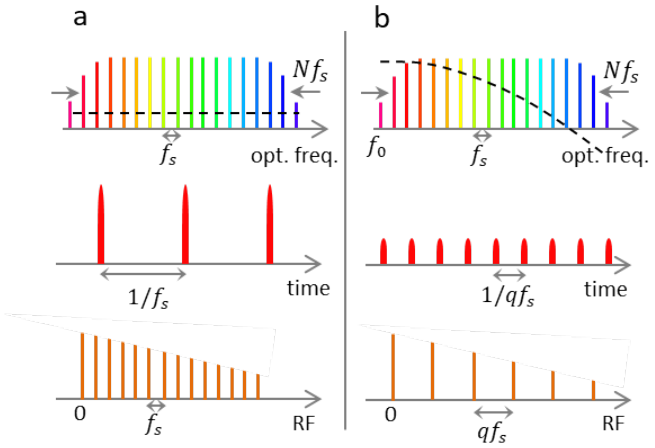

Fig. 1. a: From top to bottom: optical spectrum of a ML frequency comb (FSR: f_s), resulting pulse train (rep. rate: $1/f_s$), and intensity spectrum (power spectrum of the photo-current). The spectral phase of the ML frequency comb (dashed line) is flat (or linear). b: Case of an optical frequency comb set in a fractional Talbot condition. The spectral phase is quadratic (the phase of the comb line labeled by n is $-\pi\frac{p}{q}n^2$, see text). The repetition is qf_s (here, $q = 3$), similar to the spacing of the intensity spectrum.

A. Phase noise of a mode-locked frequency comb

First, we assume that the input frequency comb is mode-locked, i.e. all complex amplitudes of the comb lines have a linear spectral phase (Fig. 1 a). As said, a constant or linear spectral phase term does not change the phase properties of the beatnote at qf_s. For this reason, without loss of generality, we can assume that this phase is equal to zero. Therefore the E_n terms are real, and the phase noise of the beatnote at frequency qf_s can be written as:

$$\psi_q(t) \approx \tan(\psi_q(t)) = \frac{\sum_{n=q}^{N} E_n E_{n-q}(\phi_n(t) - \phi_{n-q}(t))}{\sum_{n=q}^{N} E_n E_{n-q}} \quad (5)$$

or, equivalently:

$$\psi_q(t) = \sum_{n=0}^{N} c_n \phi_n(t), \quad (6)$$

where:

- for: $0 \leqslant n < q$, $c_n = -\frac{E_{n+q}E_n}{\sum_{n=q}^{N} E_n E_{n-q}}$
- for: $q \leqslant n \leqslant N-q$, $c_n = \frac{E_n E_{n-q} - E_{n+q}E_n}{\sum_{n=q}^{N} E_n E_{n-q}}$
- for: $N-q < n \leqslant N$, $c_n = \frac{E_n E_{n-q}}{\sum_{n=q}^{N} E_n E_{n-q}}$.

In the case where the phase fluctuations of all individual comb lines are identical, the phase noise of the beating at qf_s reduces to zero, due to the cancellation of the phase terms in the sum.

In the opposite case where all phase fluctuations of the comb lines are statistically independent, the power spectral density (PSD) of the phase noise $\psi_q(t)$, defined by: $|\tilde{\psi}_q(f)|^2 = \lim_{T\to\infty} \frac{|\int_0^T \psi_q(t)e^{-i2\pi ft}dt|^2}{T}$ writes:

$$|\tilde{\psi}_q(f)|^2 = \sum_{n=0}^{N} c_n^2 |\tilde{\phi}_n(f)|^2, \quad (7)$$

where $|\tilde{\phi}_n(f)|^2$ is the PSD of $\phi_n(t)$. Here, we use the property that the PSD of a sum of statistically independent random processes is equal to the sum of PSD of the individual processes.

B. Phase noise of a frequency comb in a temporal Talbot condition

The intensity of a ML frequency comb contains frequency components multiples of the fundamental frequency f_s. Thus, in principle, a ML laser can be used as a source of RF sine waves at multiples of f_s. However in practice, obtaining a single tone signal requires to filter out all other frequency components that appear in the intensity. Moreover, in several applications like photonic sampling where pulses are needed, ML lasers provide only pulse trains at the fundamental frequency f_s. As discussed in the introduction, this brings an important limitation to the generation of reconfigurable pulse trains with high repetition rate, and low phase noise. On the contrary, fractional Talbot effect is an attractive strategy to generate pulses at a repetition rate equal to a multiple of the comb FSR, without resorting to spectral filtering. As said, the essence of Talbot effect, is to apply a quadratic spectral phase onto a ML frequency comb. More precisely, it can shown that when the spectral phase of the comb is set in such a way that: $E_n = |E_n|e^{-i\pi\frac{p}{q}n^2}$, then the resulting intensity consists of a train of transform limited pulses, at the repetition rate qf_s (Fig. 1 b) [16], [17].

In this case, $E_n E_{n-q}^{*} = |E_n E_{n-q}|e^{-i\pi\frac{p}{q}(2nq-q^2)} = |E_n E_{n-q}|e^{i\pi pq}$. Since the phase term is independent of n, it can be discarded, and the beatnote at frequency qf_s simply writes:

$$\tilde{I}_q(t) = \sum_{n=q}^{N} |E_n E_{n-q}|\Big(1 + i(\phi_n(t) - \phi_{n-q}(t))\Big). \quad (8)$$

The expression of $\tilde{I}_q(t)$ is similar to the one obtained in the case of the ML laser, and Eq. 6 is still valid, provided one replaces E_n by $|E_n|$.

III. Phase Noise of Talbot Lasers: Theoretical Aspects

In this section, we investigate the specific case of Talbot lasers. As said, they differ substantially from a mode-locked frequency comb in a temporal Talbot condition, since the quadratic spectral phase is induced simultaneously with the creation of the frequency comb. In these systems, due to the specific process of the comb generation by successive roundtrips in a FSL, the relationships between the phase fluctuations of the comb lines can be described in a closed form. First, we recall the principle of a Talbot laser. Then we consider the two sources of phase fluctuations: (i) the phase fluctuations that occur in the injection arm, and (ii), the phase fluctuations in the loop itself. In both cases, we obtain a phase noise transfer function, by proving that the phase noise PSD of the pulse train at qf_s is equal to the product of a frequency-dependent function, by the PSD of the phase fluctuations.

A. Generalities of Talbot lasers

Recall that a Talbot laser is a cavity (or a loop) containing a frequency shifter, a gain medium, and seeded by a CW laser (Fig. 2 a) [27]. In most cases, the frequency shifter is based on acousto-optic interaction in a Bragg cell (i.e. ensured by an AOFS, or acousto-optic frequency shifter). Each time a photon makes a roundtrip in the cavity, it experiences a frequency shift equal to the frequency of the acoustic wave in the case of a ring cavity (or a loop), or to twice the acoustic frequency in the case of a linear cavity. An input coupler enables to seed the FSL by a monochromatic laser, and a second one to extract a fraction of the light inside the loop. To compensate for the losses of the cavity, an optical amplifier is inserted. In practice, an optical tunable bandpass filter (TBPF) is also added, in order to control the comb spectral bandwidth, and to limit the ASE emitted by the gain medium. The spectrum of the light at the FSL output is a comb of optical frequencies, starting at f_0, the frequency of the seed laser, and spaced by f_s, the frequency shift per roundtrip (Fig. 2 b). Contrary to regular laser cavities, the cavity does not play any spectral selection process, and a competition occurs in Talbot lasers, between the coherent frequency comb, and the ASE [31]. To limit the ASE and favor the comb regime, Talbot lasers usually operate just below laser threshold. In practice, it is possible to obtain more than $N = 1000$ mutually coherent spectral lines with a flatness of a few dB [30]. In the absence of phase fluctuations and neglecting the ASE produced by the gain medium, it can be shown that the output electric field writes:

$$E(t) = E_0 e^{i2\pi f_0 t} \sum_{n=0}^{\infty} \eta^n e^{i2\pi n f_s t} e^{-i2\pi n f_0 \tau_c} e^{-i\pi n(n+1) f_s \tau_c}, \tag{9}$$

where τ_c is the cavity roundtrip time, and η the transmission coefficient of FSL per roundtrip. η is set by the gain and losses of the FSL. As said, in practice, η is slightly smaller than unity, to remain below the laser threshold. The amplitude of the comb lines scales as η^n, resulting in an exponential decay of the spectral envelope. Here, we have assumed for simplicity, that the expansion of the electric field in frequency components, can be extended to infinity (rather than N). The occurrence of a quadratic term in the spectral phase is at the origin of a temporal Talbot effect. More precisely, it can be shown that when f_s and τ_c satisfy the so-called fractional Talbot condition: $f_s\tau_c = p/q$, where p and q are mutually prime integers, then the output intensity consists of transform limited pulses, at repetition rate given by the relation $qf_s = p/\tau_c$.

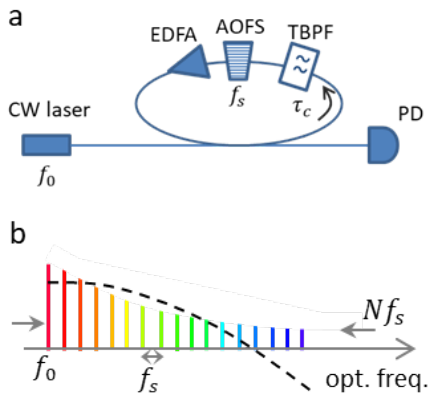

Fig. 2. a: Sketch of a fiber Talbot laser. A CW monochromatic laser (frequency: f_0) injects a frequency shifting loop (FSL), containing a tunable bandpass filter (TBPF), an acousto-optic frequency shifter (AOFS) driven at f_s, and an erbium-doped fiber amplifier (EDFA). The output intensity is detected by means of a photodiode (PD). b: Optical spectrum at the FSL output. The comb (FSR: f_s) shows an exponentially decaying envelope. The spectral phase (dashed line) is quadratic. The spectral width of the comb, denoted Nf_s, is set by the TBPF.

Talbot lasers (or FSLs) are a simple platform for generating transform-limited pulses at a repetition rate easily tunable over several orders of magnitude, by a simple adjustment of one of the system's parameters, f_s and τ_c. In the following, we provide an extensive characterization of the phase noise in Talbot lasers, and show that under reasonable assumptions, it is possible to derive analytically a transfer function from the PSD of the sources of phase noise, to the PSD of the phase noise at the repetition rate (qf_s) set by the Talbot condition.

B. Phase noise transfer function in Talbot lasers

To derive an analytic expression of the noise transfer function, we broadly divide the noise source into two contributions, namely, (i) the phase fluctuations on the electric field before its injection in the loop termed as $\phi(t)$, and (ii) the fluctuation in phase inside the loop represented by $\varphi(t)$. The former originate from the phase noise of the seed laser itself, or to a lesser extent, from fluctuations of the injection fiber's length. The later is attributed to the length fluctuations of the loop, as well as the phase fluctuations induced by the frequency shifter. Its worth noting that $\phi(t)$ and $\varphi(t)$ have a different nature and are expected to play a different role on the phase noise of the output pulse train, for instance, the first one only affects the injection electric field (Fig. 3), while the second one is accumulated by the light at each roundtrip in the FSL.

1) Phase fluctuations in the injection arm: Assuming that the phase fluctuations in the injection arm can be described by the function $\phi(t)$, the output electric field writes:

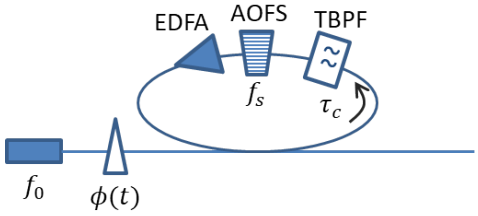

Fig. 3. The phase fluctuations in the injection arm (fiber length, phase noise of the injection laser) are modeled by a variable phase $\phi(t)$.

$$E(t) = E_0 e^{i2\pi f_0 t} \times \sum_{n=0}^{\infty} \eta^n e^{i2\pi n f_s t} e^{-i2\pi n f_0 \tau_c} e^{-i\pi n(n+1) f_s \tau_c} e^{i\phi(t-n\tau_c)}. \quad (10)$$

The calculations derived in the previous section are valid, provided that E_n is replaced by $\eta^n E_0$, and $\phi_n(t)$ by $\phi(t-n\tau_c)$. Then, according to Eq. 3, the phase $\psi_q(t)$ of the beatnote at qf_s writes:

$$\psi_q(t) = (1-\eta^2) \sum_{n=q}^{\infty} \eta^{2n-2q} (\phi(t-n\tau_c) - \phi(t-(n-q)\tau_c)). \quad (11)$$

The Fourier transform of the phase noise writes: $\tilde{\psi}_q(f) = \int \psi_q(t) e^{i2\pi f t} dt$. Therefore:

$$\tilde{\psi}_q(f) = (1-\eta^2)\tilde{\phi}(f) \sum_{n=q}^{\infty} \eta^{2n-2q} (e^{i2\pi n f \tau_c} - e^{i2\pi (n-q) f \tau_c}), \quad (12)$$

and:

$$\tilde{\psi}_q(f) = (1-\eta^2)(1-e^{-i2\pi q f \tau_c})\tilde{\phi}(f) \sum_{n=q}^{\infty} \eta^{2n-2q} e^{i2\pi n f \tau_c}. \quad (13)$$

Finally,

$$\tilde{\psi}(f) = \frac{(1-\eta^2)(e^{i2\pi q f \tau_c} - 1)}{1-\eta^2 e^{i2\pi f \tau_c}} \tilde{\phi}(f) = H_q(f)\tilde{\phi}(f). \quad (14)$$

The phase noise PSD of the output pulse train at qf_s writes:

$$|\tilde{\psi}_q(f)|^2 = |H_q(f)|^2 |\tilde{\phi}(f)|^2 = 4 \frac{(1-\eta^2)^2 \sin^2(\pi q f \tau_c)}{1 - 2\eta^2 \cos(2\pi f \tau_c) + \eta^4} |\tilde{\phi}(f)|^2. \quad (15)$$

This relation evidences in a straightforward manner the transfer function of the FSL, between the phase fluctuations on the injection arm, and the phase noise of the output pulse train. The square modulus of the transfer function is plotted in Fig. 4 for different values of the parameters η and q. The transfer function shows the following features:

- The transfer function is periodic (spectral period: $1/\tau_c$), and vanishes at frequencies multiples of $1/(q\tau_c)$ (including at null frequency, and at multiples of $1/\tau_c$).
- The transfer function vanishes when $f \to 0$. This interprets as the fact that if the phase fluctuations $\phi(t)$ are much slower than the photon lifetime in the loop, one has, $\phi(t-n\tau_c) \simeq \phi(t)$ for any value of $n < N$. Then the phase term $e^{i\phi(t-n\tau_c)}$ can be replaced with $e^{i\phi(t)}$ in Eq. 10, factorized, and finally discarded, since it is a pure phase term in the expression of the electric field.
- The system shows a filtering effect of the phase noise between multiples of $1/\tau_c$. The quality of the filtering of the phase noise increases with η, i.e. with the number of comb teeth.
- In the vicinity of multiples of $1/\tau_c$, i.e. when $f \simeq k/\tau_c$ (k integer), one has:

$$|\tilde{\psi}_q(f)|^2 \simeq (2\pi q(f\tau_c - k))^2 |\tilde{\phi}(f)|^2. \quad (16)$$

  Here, the square modulus of the transfer function increases as f^2. For a given offset frequency, it scales as q^2. Therefore, in a logarithmic scale, $\mathcal{L}(f)$, defined by $10\log|\psi_q(f)|^2$, increases as $20\log q$. This result is identical to what is encountered in analog frequency multiplication: ideal analog multiplication of the frequency of a single tone signal by factor of q leads to an increase of the phase noise power spectral density (PSD) of $20\log q$ (logarithmic scale) [1] [32].
- For offset frequencies far from multiples of $1/\tau_c$, since the $\sin^2(\pi q f \tau_c)$ term varies with frequency much faster than the denominator $1 - 2\eta^2\cos(2\pi f\tau_c) + \eta^4$, one can average the numerator, and the noise PSD rewrites:

$$|\tilde{\psi}_q(f)|^2 \simeq 2 \frac{(1-\eta^2)^2}{1 - 2\eta^2 \cos(2\pi f \tau_c) + \eta^4} |\tilde{\phi}(f)|^2, \quad (17)$$

  which proves that the phase noise PSD, on average, does not depend on q, the multiplicative factor.

This last result differs substantially from analog frequency multiplication. This specific property directly arises from the specific relation between the phase fluctuations of the comb teeth in the FSL, set by the generation process of the comb itself.

2) Phase noise in the FSL: We now turn to the influence on the phase noise of the pulse train, of phase fluctuations occurring inside the loop (Fig. 5). As said, these phase fluctuations can originate from variations in the length of the loop (vibrations, thermal drifts), or from phase noise on the RF signal driving the frequency shifter. Notice that here, we do not consider the role played by the ASE of the amplifier. It can be shown that the ASE is not a multiplicative, but an additive noise [33]. Therefore, it cannot be treated similarly to the other sources of (multiplicative) noise described here. The specific role played by the ASE is discussed in section IV.C.

We define $\varphi(t)$, the temporal fluctuations of the phase occurring inside the loop. Unlike the previous case, the

[1]Consider a complex signal $s(t)$ at frequency f_0, showing phase fluctuations $\psi(t)$. One has: $s(t) \propto e^{i2\pi f_0 t + i\psi(t)}$. The phase noise PSD writes $|\tilde{\psi}(f)|^2$. Analog frequency multiplication by q generates a signal $s_q(t) \propto e^{i2\pi q f_0 t + iq\psi(t)}$, whose phase noise PSD writes: $|\tilde{\psi}_q(f)|^2 = q^2|\tilde{\psi}(f)|^2$. On a logarithmic scale, the PSDs are shifted by $20\log q$.

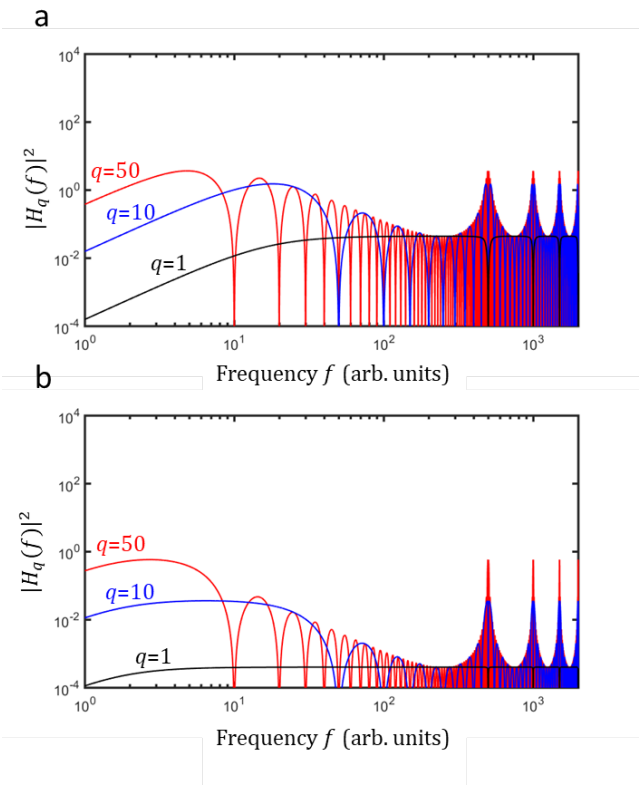

Fig. 4. Square modulus of the noise transfer function (i.e. $|\tilde{\psi}_q(f)|^2/|\tilde{\phi}(f)|^2$) as a function of the offset frequency f (in arb. units) for phase fluctuations in the injection arm. In the simulations, $1/\tau_c = 500$, $\eta = 0.95$ (resp. 0.99) in a (resp. b). Black: $q = 1$, blue: $q = 10$, red: $q = 50$.

phase fluctuations in the loop accumulate over the successive roundtrips, in the phase of the electric field.

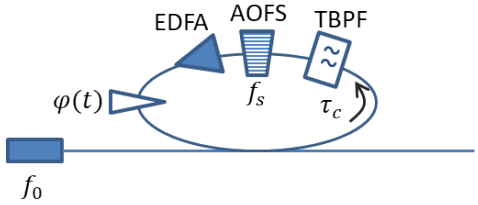

Fig. 5. The phase fluctuations in the loop (fiber length, phase noise of the frequency shifter) are modeled by a random function $\varphi(t)$.

The electric field at the FSL output writes:

$$E(t) = E_0 e^{i2\pi f_0 t} \times \sum_{n=0}^{\infty} \eta^n e^{i2\pi n f_s t} e^{-i2\pi n f_0 \tau_c} e^{-i\pi n(n+1) f_s \tau_c} e^{i\theta_n(t)}, \quad (18)$$

where :

- $\theta_0(t) = 0$,
- $\theta_{n>0}(t) = \sum_{k=0}^{n-1} \varphi(t - k\tau_c)$.

Owing to the previous calculations, the phase fluctuations $\psi_q(t)$ of the pulse train at qf_s can be expressed, by replacing formally E_n by $\eta^n E_0$, and $\phi_n(t)$ by $\theta_n(t)$. Assuming that the accumulated phase fluctuations are small ($\theta(t) \ll 2\pi$), $\psi_q(t)$ writes:

$$\psi_q(t) = (1-\eta^2) \sum_{n=q}^{\infty} \eta^{2n-2q} (\theta_n(t) - \theta_{n-q}(t)). \quad (19)$$

Defining $|\varphi(f)|^2 = \lim_{T\to\infty} \frac{|\int_0^T \varphi(t) e^{-i2\pi f t} dt|^2}{T}$, calculations similar to the case of fluctuations occurring in the injection arm lead to the following expression of the phase noise PSD of the pulse train at qf_s:

$$|\tilde{\psi}_q(f)|^2 = \frac{(1-\eta^2)^2}{1 - 2\eta^2 \cos(2\pi f \tau_c) + \eta^4} \frac{\sin^2(\pi q f \tau_c)}{\sin^2(\pi f \tau_c)} |\tilde{\varphi}(f)|^2. \quad (20)$$

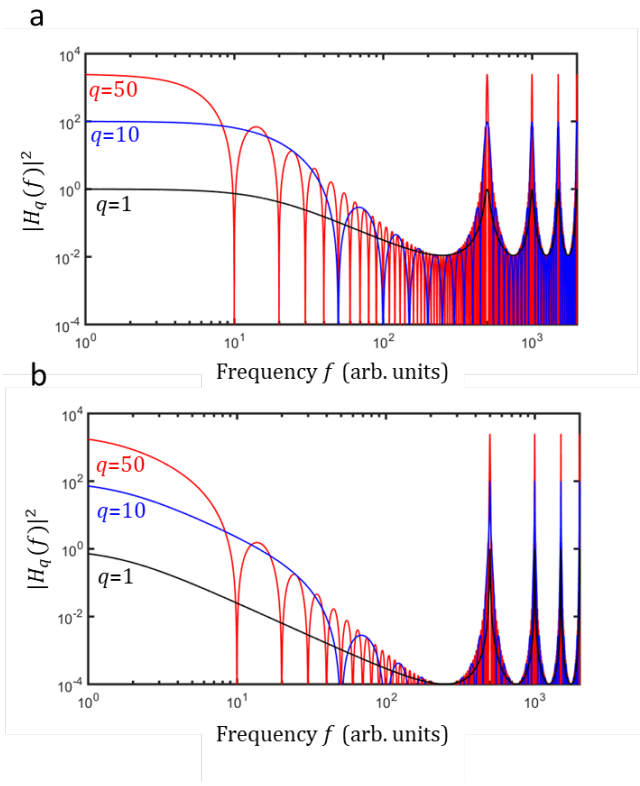

Fig. 6. Square modulus of the noise transfer function (i.e. $|\tilde{\psi}_q(f)|^2/|\tilde{\varphi}(f)|^2$) as a function of the offset frequency f (in arb. units) for phase fluctuations in the loop. In the simulations, $1/\tau_c = 500$, $\eta = 0.95$ (resp. 0.99) in a (resp. b). Black: $q = 1$, blue: $q = 10$, red: $q = 50$.

Similarly to the case of phase fluctuations occurring in the input arm, the PSD of the phase noise of the output pulse train is proportional to the PSD of the phase fluctuations occurring in the FSL. But contrary to the previous case, the transfer function for phase fluctuations occurring inside the loop does not vanish at multiples of $1/\tau_c$, where it is maximal (Fig. 6). Moreover, its modulus can strongly exceed unity, due to the fact that depending on their frequency, the fluctuations can be amplified by the loop. The transfer function displays other features similar to the case of phase fluctuations on the injection arm:

- The noise transfer function vanishes at frequencies multiples of $1/(q\tau_c)$ (excepted at multiples of $1/\tau_c$).
- In the vicinity of multiples of $1/\tau_c$, one has:

$$|\tilde{\psi}_q(f)|^2 \simeq q^2|\tilde{\varphi}(f)|^2. \quad (21)$$

The phase noise PSD increases as q^2. In a logarithmic scale, $\mathcal{L}(f)$ increases as $20\log q$, a result similar to the case of phase fluctuations in the injection arm.
- The value of the transfer function at multiples of $1/\tau_c$ does not depend of η. Moreover, similarly to the previous case, the quality of the filtering of the phase noise increases with η, i.e. with the number of comb teeth.
- In frequency regions far from multiples of $1/\tau_c$, similarly to the previous case, the noise transfer function can be averaged, so that:

$$|\tilde{\psi}_q(f)|^2 \simeq \frac{(1-\eta^2)^2}{1-2\eta^2\cos(2\pi f\tau_c)+\eta^4}\frac{1}{2\sin^2(\pi f\tau_c)}|\tilde{\varphi}(f)|^2. \quad (22)$$

Again, this expression does not depend on q, which shows that the phase noise PSD, in average, is independent from q, the multiplicative factor.

IV. Phase noise of Talbot lasers: experimental results

In this section, we experimentally characterize the phase noise properties of a Talbot laser, submitted to external noise sources in both the injection arm and in the FSL itself. The results turn out to show a good agreement with the theoretical predictions described previously. In particular, we evidence the fact that the phase noise evolves as $20\log q$ for low offset frequencies, and that it is independent of q at high offset frequencies.

A. Parameters of the Talbot laser

The Talbot laser used in these experiment is based on a polarization-maintaining fiber loop. It contains an EDFA, a fiber frequency shifter driven around 80 MHz, and a tunable optical bandpass filter. The roundtrip time in the loop is found to be equal to $\tau_c = 214.928$ ns. (This value can be inferred by setting the system in an integer Talbot condition, i.e. $q = 1$. The value of f_s is precisely adjusted, so as to maximize the peak power of the pulses. Then, the precise value of τ_c is obtained by utilizing the Talbot condition: $qf_s = p/\tau_c$.) The FSL is seeded by a commercial CW fiber laser at 1550 nm (1 kHz linewidth, injected power: ~ 9 μW) by means of a 3 dB X-coupler. The other port of the coupler enables to extract a fraction of the optical field circulating in the loop. The output intensity is measured by a fast photodiode (18 ps-risetime), and the photocurrent is sent to a phase noise analyzer.

B. Phase noise of the Talbot laser

In the first set of experiments, we characterize the phase noise in different Talbot conditions. To do so, the length of the fiber loop (i.e. τ_c) is kept constant, and the value of f_s is adjusted, in order to reach fractional Talbot conditions of the form $f_s\tau_c = p/q$ for different values of p and q. We consider the following sets of values: $f_s = 80.0267$ MHz ($p = 86, q = 5$), $f_s = 81.0199$ MHz ($p = 504, q = 29$), and $f_s = 81.3057$ MHz ($p = 1763, q = 101$), among others. The repetition rates of the pulse trains (i.e. qf_s) are respectively equal to: 400.1 MHz, 2.350 GHz, and 8.211 GHz. In Fig. 7a, we plot the intensity spectra (i.e. the power spectrum of the photocurrent) recorded at the output of the FSL for each of these Talbot conditions. Notice that the spectrum contains harmonics of qf_s (according to Fig. 1b), and residual beatnotes at harmonics of f_s [27]. Then, we compare the phase noise PSD in different Talbot conditions. As said, the phase noise arises from phase fluctuations in both the injection arm, and in the loop itself. The results are displayed on Fig. 7b. According to the theoretical predictions, the phase noise increases with q at low offset frequencies. However, at higher offset frequencies (> 100 kHz), the phase noise is almost constant (independent of q). The optical power at the photodiode is 800 μW. The responsivity of the photodiode is 0.9 A/W, which results in a shot noise PSD of -150 dBc/Hz. The slight increase of the noise floor (< 5 dB) for $q = 101$ is due to the decrease of the RF input power at frequency qf_s, an effect apparent in Fig. 7a. As expected, the phase noise show peaks at offset frequencies multiples of $1/\tau_c$ (= 4.66 MHz). Moreover, according to Eq. 15, and Eq. 20, the phase noise PSD shows dips at offset frequencies multiples of $1/q\tau_c$. (In the case where $q = 5$, supernumerary dips occur, whose origin is not clearly understood yet.) Notice also that all PSD curves show excess noise at low offset frequencies, likely due to the phase noise of the seed laser.

To clearly evidence the dependence of the phase noise with q at low- and high- offset frequency, we plot in Fig. 7c the phase noise PSD averaged from 10^3 to 10^4 Hz (i.e. the low frequency), and from 3.10^5 to 3.10^6 Hz (the high frequency part), for Talbot conditions ranging from $q = 5$, to $q = 101$. The plots clearly shows that the phase noise at low offset frequencies evolves as $20\log(q)$, similarly to analog multiplication, and is then constant at high offset frequencies. Finally, we plot in Fig. 7d the timing jitter, defined as $\sigma_J = 1/(2\pi qf_s)\sqrt{\int_{f_1}^{f_2}|\tilde{\psi}_q(f)|^2 df}$. For all values of the repetition rate (i.e. of q), the timing jitter is integrated from 100 kHz to the Nyquist frequency (i.e. $qf_s/2$) [34]. In the case where $q = 101$ (rep. rate $= 8.211$ GHz), the integrated timing jitter from 10 kHz to the Nyquist frequency is 944 fs, while it is equal to 351 fs from 100 kHz to the Nyquist frequency. Notice that the timing jitter decreases as a function of the repetition rate, a feature that differs also from the process of ideal frequency multiplication, where the timing jitter (integrated up to the Nyquist frequency) would increase with the repetition rate.

In a second set of experiments, we evidence the proportionality of the phase noise PSD in Talbot lasers, with the PSD of the phase fluctuations applied on the injection arm. This is done in order to verify experimentally Eq. 15, and to justify the existence of the transfer function. (A similar study, which has not been done for practical reasons, could have been carried out for phase fluctuations induced in the FSL).

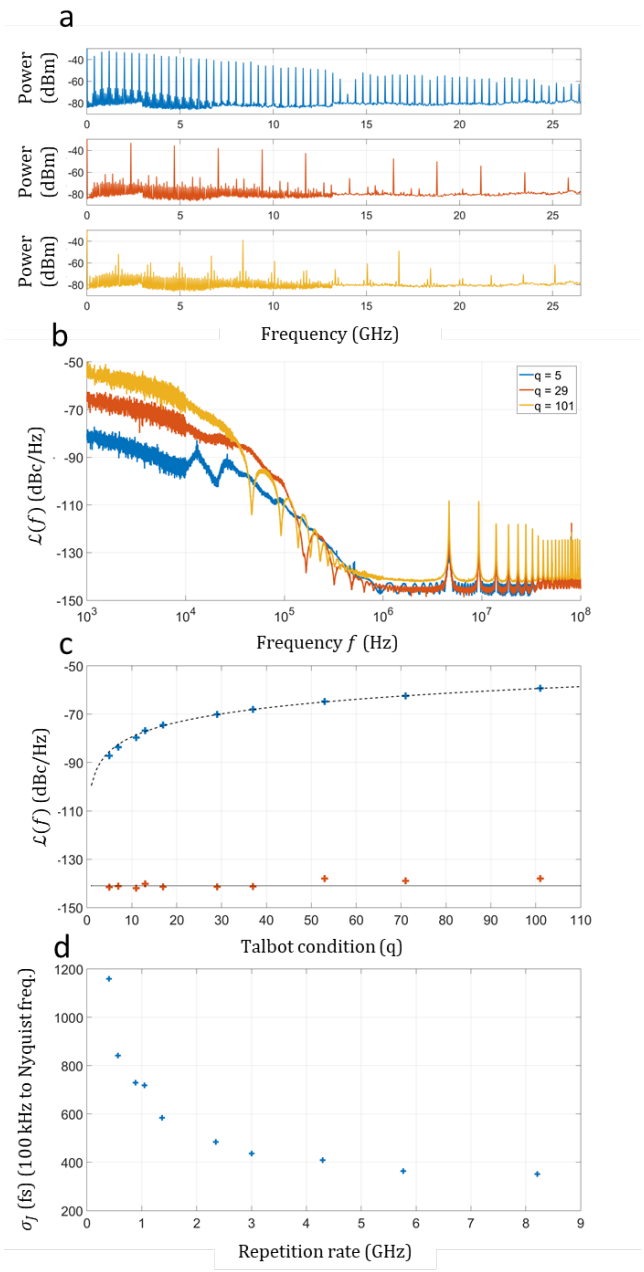

Fig. 7. a: Intensity spectra of the Talbot laser in different Talbot conditions (blue: $q = 5$, red: $q = 29$, and yellow: $q = 101$). The dip around 14 GHz is due to the photodiode response function. b: Phase noise PSD (in dBc/Hz) as a function of the offset frequency, measured for different Talbot conditions ($q = 5, 29$ and 101). c: Red (resp. blue) dots: Phase noise (in dBc/Hz) at low (resp. high) offset frequencies for different Talbot conditions ($q = 5$ to 101). The dotted and dash lines are respectively a constant PSD at -141 dBc/Hz (bottom), and the curve $\mathrm{PSD}(q) = \mathrm{PSD}(q = 1) + 20\log(q)$ (top). d: Timing jitter (in fs) as a function of the repetition rate. σ_J is integrated from 100 kHz, to the Nyquist frequency.

For this aim, we artificially degrade the phase noise of the seed laser, via a phase modulator driven by a white noise signal. We assume that the mechanical/thermal phase fluctuations of the injection fiber are negligible as compared to the phase fluctuations of the seed laser. We measure simultaneously the optical phase noise PSD on the injection arm and the corresponding electrical phase noise PSD of the pulse train, for different Talbot conditions (i.e. different values of q). The phase modulator is inserted between the seed laser, and the injection coupler. A measurement bench, based on a delayed self-heterodyne interferometer has been developed, to measure the phase noise of the narrow-linewidth laser after the phase modulation. The spectrum of the white noise signal applied to the phase modulator ranges from DC to 20 MHz (Fig. 8 a). The level of the PSD of the white noise is controlled by the peak-to-peak voltage applied to the modulator. The phase noise of the degraded seed laser measured for different values of the modulation voltage, is plotted in Fig. 8 b. The phase noise increases with the applied voltage for offset frequencies larger than 0.1 to 1 MHz. Below this value, the phase noise induced by the random phase modulation is smaller than the intrinsic phase noise of the laser. Then, we measure the phase noise of the pulse trains in different Talbot conditions (Fig. 8 c: $q = 11$, Fig. 8 d: $q = 37$). As expected, the phase noise PSD is not modified below 0.1 MHz. At higher offset frequencies, the noise level passes the noise floor and increases with the modulation voltage. Interestingly, this brings the dips at multiples of $1/q\tau_c$ well above the detection noise floor, making them clearly visible for large modulation voltages.

C. Comparison with the theoretical predictions

The comparison of the experimental results with the theoretical model provides interesting details on the different sources of noise in FSLs. Recall that the phase fluctuations that occur in the injection arm, vanish at offset frequency multiples of $1/\tau_c$. Therefore the phase noise at these frequencies come only from the phase fluctuations taking place in the FSL. Mainly, the phase fluctuations in the FSL itself have three different origins: the fluctuations of the fiber length, the phase noise of the synthesizer driving the AOFS, and the ASE emitted by the amplifier. Regarding the latter noise source, so far, in the analytical model of the phase noise, we have neglected the ASE of the amplifier and considered only multiplicative noise sources. Here, to account for the presence of the ASE in the experimental system, we assume that in first approximation, the ASE brings a constant background (white noise) to the phase noise PSD. We also make the hypothesis that the length fluctuations of the fiber are due to mechanical variations (e.g. vibrations), and thermal drifts. We assume that these fluctuations occur on times scales larger than hundreds of microsecond, and that they play a negligible role at offset frequencies larger than 10 kHz. Finally, we suppose that the dependence of the phase noise of the synthesizer with the offset frequency is same for all values of f_s. This hypothesis is justified by the fact that, in practice, f_s operates on a narrow frequency range, between 80 MHz and 82 MHz.

Owing to these three hypotheses, one can write the PSD of the phase fluctuations inside the FSL, as: $|\tilde{\varphi}(f)|^2 = a + |\tilde{\varphi}_{\mathrm{synth}}(f)|^2$, where a and $|\tilde{\varphi}_{\mathrm{synth}}(f)|^2$ are the phase fluctuations PSD of the ASE and of the synthesizer respectively. The latter can readily be measured by means of a phase noise analyzer. As said, the phase fluctuations in the injection arm play no role on the phase noise at multiples of $1/\tau_c$. Then, for any positive integer k, one has, from Eq.(21):

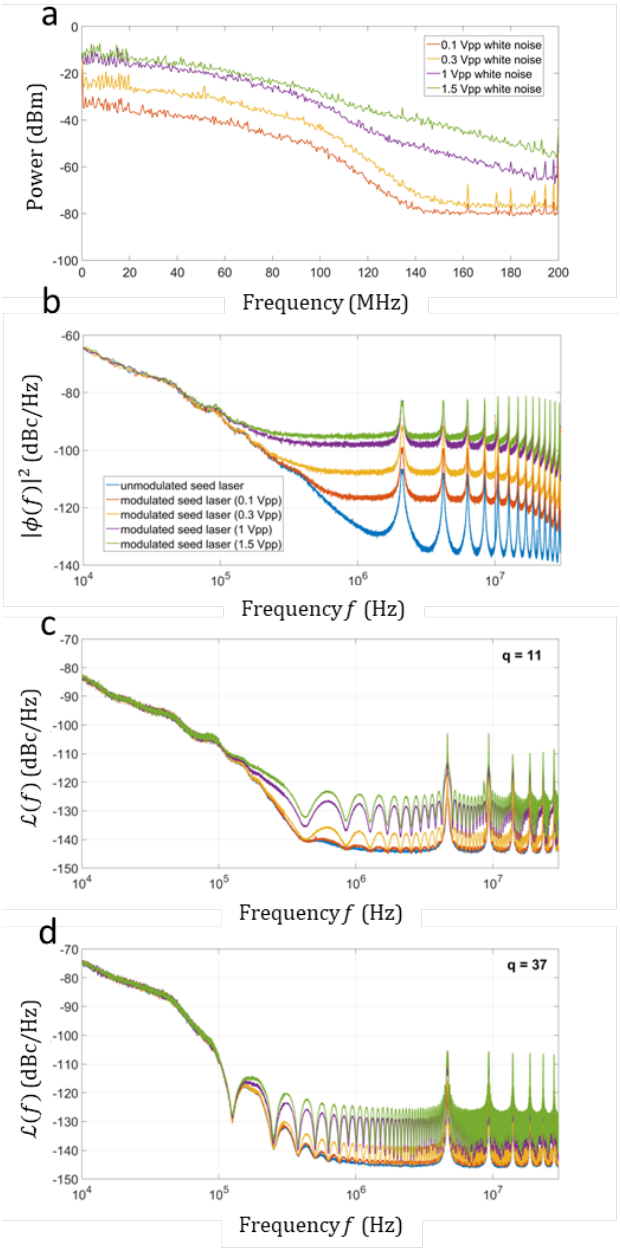

Fig. 8. a: Power spectrum of the noise signal applied to the modulator, for different values of the peak-to-peak voltage. b: Phase noise of the seed laser after modulation, measured by a delayed self-heterodyne interferometer. The coherence of the laser is degraded, owing to a phase modulation by a white noise, whose power is controlled by the peak-to-peak value of the applied voltage. The peaks at multiples of 2 MHz are experimental artefacts, due to the measurement technique itself. c (resp. d): Phase noise of the pulse train at the output of the Talbot laser for different values of the modulation voltage. The value of q is 11 (resp. 37), and the repetition rate is 884 MHz (resp. 3.001 GHz).

$$|\tilde{\psi}_q(k/\tau_c)|^2 = q^2(a + |\tilde{\varphi}_{\text{synth}}(k/\tau_c)|^2). \tag{23}$$

By measuring the value of the phase noise PSD $|\tilde{\psi}_q(k/\tau_c)|^2$ for different values of k and q, one can deduce the value of a, the PSD of the phase fluctuations due to the ASE, and get knowledge of the phase noise PSD $|\tilde{\varphi}(f)|^2$. An important parameter involved in both transfer functions is η. Since both transfer functions depend strongly on η, the latter must be determined accurately. For this aim, recall that in the range 10-100 kHz, the phase noise of the pulse train is dominated by the phase fluctuations in the injection arm, i.e. by the (degraded) phase noise of the seed laser. Since the latter can be measured experimentally, a precise value of η can be inferred using Eq. 15. In the experiments described here, one obtains $\eta = 0.9955$. Then the knowledge of η gives access to both transfer functions.

In Fig. 9a, we plot the experimental phase noise PSD (in blue) measured when $q = 37$, and with a degradation of the seed laser phase noise (1 V_{pp}). The yellow (resp. red) curve represents the PSD of the phase noise due to the phase fluctuations occurring inside the FSL (resp. in the injection arm). We added a noise floor of -145 dBc/Hz, to account for the thermal floor of the detection process. The addition of both phase noise PSDs is the purple curve in Fig. 9 a. Notice the good agreement with the experimental phase noise (in blue). Still, a slight difference between the theoretical and the experimental curves is noticeable in the region between the peaks at multiples of $1/\tau_c$. This difference is observed in different experimental conditions (value of q, phase noise of the seed laser). Yet, the origin of this difference is not completely clear. A first possibility is a slight modulation of η with the frequency. Such an effect could originate from a residual cavity effect, due to incomplete rejection of the zero diffraction order in the AOFS. We investigated this possibility, by taking into account a slight harmonic modulation of η with the frequency $1/\tau_c$ (spectral period). Taking a modulation contrast as weak as 0.5 % enables to reproduce qualitatively the experimental phase noise (red plot in Fig. 9 b). Another explanation could come from the approximation that has been made, that the ASE background produces a constant noise floor in the phase noise PSD. In reality, it has been shown that in frequency-shifted feedback (also called modeless) lasers, i.e. FSLs seeded only with the ASE of the gain medium, the output intensity is periodic (period: τ_c) [35]. Talbot lasers are systems where the incoherent (i.e. modeless) behavior cannot be neglected, and competes with the coherent one (i.e. the optical frequency comb) [36]. This argument would justify the existence of $1/\tau_c$-periodic modulation of the ASE intensity spectrum, and contradict the aforementioned hypothesis of white ASE noise. A last reason for this discrepancy could also be the relative intensity noise of the seed laser, that has been neglected in our model.

V. Reduction of the Low-Frequency Phase Noise by Locking Techniques

A remarkable feature of Talbot lasers, that differs from analog frequency multiplication processes, is the fact that at high offset frequencies, the phase noise becomes independent from the repetition rate. Typical values of the phase noise at high offset frequencies (above 10^6 Hz) approach -140 dBc/Hz for a repetition rate of 8 GHz, just above the thermal detection floor (-145 dBc/Hz). Provided one can increase the output power of the Talbot laser, this leads to the possibility of reaching very small values of RMS jitter, since the latter

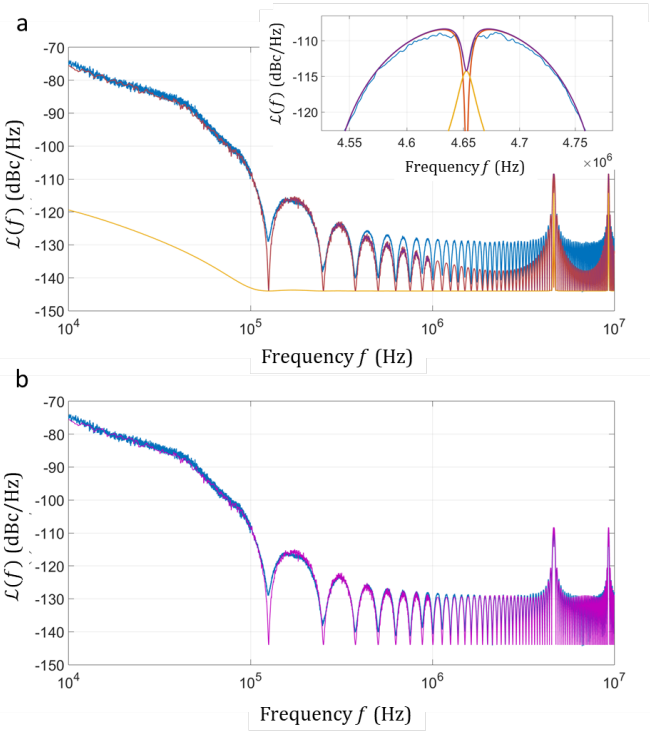

Fig. 9. a: In blue, experimental phase noise when $q = 37$. The seed laser is phase-modulated by a white noise signal (1 V_{pp}). The yellow (resp. red) curve is the contribution of phase fluctuations occurring inside the FSL (resp. in the injection arm), see text. The purple curve is the resulting expected phase noise PSD (sum of the yellow and the red curves), after determination of the experimental parameters (ASE and η). The inset provides a magnification of the peak around the offset frequency of 4.65 GHz. b: Comparison of the experimental phase noise PSD (in blue), with the expected one (purple), by taking into account a slight dependence of η with the frequency (see text).

is inversely proportional to the repetition rate. However, the phase noise at low offset frequencies increases significantly and can reach values as high as -50 dBc/Hz at 1 kHz offset frequency (rep. rate = 8 GHz). This value can be attributed to two main factors: the phase noise of the seed laser, and the mechanical and thermal drifts of the fiber. Since the phase noise at low offset frequencies increases as $20 \log q$, these noise terms become strongly amplified for large values of q. In this section, owing to a simple model for low frequency phase fluctuations, we describe an efficient technique to reduce considerably the phase noise at low frequency.

A. Theoretical aspects of the low frequency noise

In this study, we restrict to the case of phase fluctuations slower that $N\tau_c$. Again, the phase fluctuations can be separated in two contributions: $\phi(t)$ and $\varphi(t)$, the phase fluctuations in the injection arm and in the loop, respectively. As explained above, the effect of slowly-varying phase fluctuations on the injection arm can be discarded. This corresponds to the fact that the associated transfer function vanishes when the offset frequency tends to 0. On the other hand, the phase fluctuations that occur in the loop itself play an important role. We use here the formalism developed in section 3. If one assumes that these fluctuations are sufficiently slow so that, for any value of $n < N$, $\varphi(t - n\tau_c) \simeq \varphi(t)$, one can write: $\theta_n(t) = n\varphi(t)$, and the electric field rewrites:

$$E(t) = E_0 e^{i2\pi f_0 t} \times \sum_{n=0}^{\infty} \eta^n e^{i2\pi n f_s t} e^{-i2\pi n f_0 \tau_c} e^{-i\pi n(n+1) f_s \tau_c} e^{in\varphi(t)}. \quad (24)$$

Then, the envelope of the beatnote at frequency qf_s is given by:

$$\tilde{I}_q(t) = \Big(\sum_{n=q}^{N} \eta^{2n-q} \Big) e^{iq(\varphi(t) - 2\pi f_s \tau_c - 2\pi f_0 \tau_c)}, \quad (25)$$

and the phase of $\tilde{I}_q(t)$ at frequency qf_s writes:

$$\psi_q(t) = q(\varphi(t) - 2\pi f_s \tau_c - 2\pi f_0 \tau_c). \quad (26)$$

This expression shows that the phase fluctuations $\varphi(t)$ can be compensated by slightly modulating one of the three parameters f_0, f_s, and τ_c. Interestingly, the phase of the beatnote q is proportional to q. This means that if by some locking mechanism, one can fully compensate the phase fluctuations of the beatnote q, then the phase fluctuations of all other beatnotes can be canceled. Since all frequency components of the output intensity remain phase-locked, the output signal still consists of a train of transform-limited pulses. This property is important in the context of photonic-assisted sampling, where pulses with high peak power are desired.

B. Experimental results

In this part, we describe different locking schemes used to reduce the low frequency phase noise in Talbot lasers. Among the three parameters that can be used to compensate for the phase fluctuations occurring inside the loop (i.e. f_0, f_s, and τ_c), we choose to apply a feedback on f_s. This choice is motivated by simplicity: applying a phase or a frequency modulation on the frequency of the seed laser f_0 would require the use of a phase modulator, or of an acousto-optic frequency shifter. Similarly, tuning of τ_c could be achieved at the expense of a phase modulator, or of an piezo-electric fiber stretcher. On the contrary, modulation of f_s does not require any additional optical hardware, but can be achieved in a commercial function generator with an external frequency modulation input.

We investigated a locking mechanism inspired by phase-locked loops techniques. Phase fluctuations that occur inside the loop induce phase fluctuations of the optical comb lines and consequently, of the beatnotes between the comb lines. By comparing the frequency of such a beatnote to an external oscillator, we generate an error signal, proportional to the difference between the two frequencies. This error signal is processed through a standard PID (Proportional Integral Derivative) controller, and the correction signal is used to modulate in frequency the signal that drives the AOFS inside the loop, a scheme equivalent to phase-locked loops. In the specific case of FSLs, we investigated two locking mechanisms. The first one is directly derived from regular heterodyne interferometry and requires additional optical hardware (Fig.

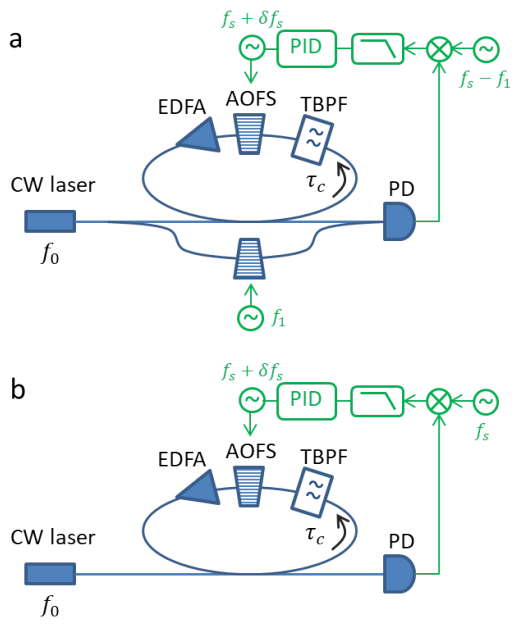

Fig. 10. a: Locking scheme on the first comb tooth (see text). The green lines are electric circuitry and components. b: Locking scheme on the first harmonic of the pulse train.

10a). It is based on the measurement of the relative phase between the reference RF oscillator, and the heterodyne signal obtained by the interference of light having experienced one round-trip in the loop, and the laser output. For this aim, the seed laser output is separated in two parts. One is sent to the FSL, the second one is frequency-shifted in a reference arm, and recombined with the FSL output. Notice that in this case, the reference arm has to be as compact and stable as possible, to consider that the phase variations measured at the output of the interferometer, are only due to the phase fluctuations occurring in the FSL $\varphi(t)$. As said, the relative phase between the two signals is used as an error signal. The latter is processed by means of the PID controller, and is applied as an external modulation to the frequency of the AOFS.

The second locking mechanism is simpler in terms of optical hardware, and consists of measuring the relative phase between a reference RF signal at f_s (in our case, close to 80 MHz), with the intensity signal (Fig. 10b). Even if the repetition rate of the output pulse train in a fractional Talbot condition is qf_s (i.e. the intensity spectrum consists of beatnotes multiples of qf_s, such as in Fig. 1b and Fig. 7a), there are unavoidable contributions in the intensity at all multiples of f_s. This is due to imperfect canceling of the beatnotes at frequencies kf_s (k integer and $k \neq q$) in the case of an optical spectrum with an exponentially decreasing envelope, such as the one encountered in FSLs [27]. Similarly to the previous case, the relative phase is used as an error signal, processed, and used to modulate the frequency of the AOFS in the FSL.

The influence of the locking on the phase noise for different Talbot conditions has been extensively studied. In both cases, the phase noise in the offset frequency range 10 Hz - 5 kHz is strongly reduced by the locking. This frequency range is set by the limitations of the PID controller. The reduction in phase noise can exceed 20 dB from 10 Hz to 1 kHz. The results obtained by means of the second locking mechanism are shown in Fig. 11.

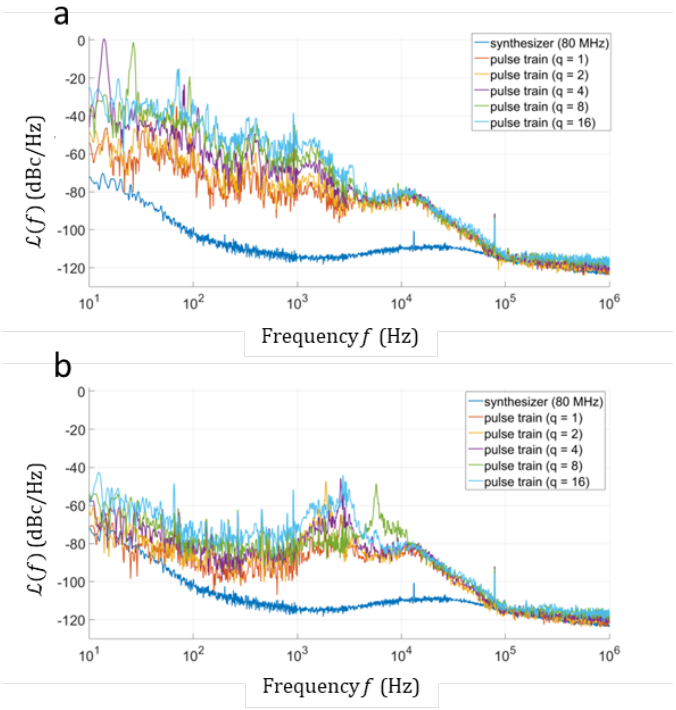

Fig. 11. a (resp. b): phase noise in different Talbot conditions without (resp. with) feedback. The error signal comes from the relative phase between a reference RF signal and the first harmonic of the pulse train intensity.

VI. Summary and Conclusion

In this article, we have provided a theoretical model and an experimental validation of the phase noise properties in Talbot lasers. Despite its simplicity, our model provides predictions in excellent agreement with the experimental results. We have restricted ourselves to multiplicative sources of phase noise, and we have neglected the influence of the gain medium dynamics, and the amplitude noise of the comb lines. Additionally, we have not taken into account additive noise sources, such as the ASE of the gain medium [33]. Among the specific features of Talbot lasers, we have proven that the phase noise of the output pulse train in a fractional Talbot condition, is related to the phase fluctuations of the system by two transfer functions. One sets the proportionality relation of the output phase noise with the fluctuations occurring in the injection arm (phase noise of the seed laser and, to a lesser extent, length variations of the injection fiber), and the second one with the fluctuations in the loop itself (phase noise of the frequency shifter, length variations of the loop). Besides intrinsic difference, the two transfer functions share common features, such as the fact that the phase noise of the output pulse train evolves as $20 \log q$ at low offset frequencies from the carrier, and is independent from the multiplicative factor at higher offset frequencies. As such, this result is remarkable, and differs substantially from

conventional cases, such as analog frequency multiplication. Therefore, Talbot lasers are a promising solution for the generation of short transform-limited pulses, at repetition rates tunable over several orders of magnitude.

At this point, it is relevant to compare Talbot lasers with HML lasers. In HML lasers, the low offset frequency phase noise of the pulse train follows the synthesizer's characteristics [13]. In practice, the synthesizer's signal is obtained by electronic multiplication of a lower frequency reference signal, and is accompanied by a increase of the phase noise by $20 \log q$. In Talbot lasers, a similar phase noise degradation with the repetition rate is observed for low offset frequencies. However, Talbot lasers are much less demanding in terms of electronic hardware, since the frequency multiplication is not realized in the synthesizer, but in the optical system by the Talbot effect itself. Instead of the multi-GHz synthesizer required in HML lasers, Talbot lasers only require a much simpler oscillator at $\sim$100 MHz. Moreover, the very architecture of Talbot lasers offers the possibility to lock the phase noise onto the low-frequency reference signal, a possibility that HML lasers do not offer. A high offset frequencies, the phase noise in HML is filtered by the cavity and is no longer constrained by the synthesizer [13], a feature related to the independence of the phase noise with the multiplication factor encountered in Talbot lasers.

In terms of ultimate phase noise performance, Talbot lasers do not reach yet the level of HML lasers. One of the reasons for this might be the ASE, that adds to the coherent pulse train. It has been shown that, in the absence of any spectral filtering mechanism, the total power of the ASE can be comparable to, or exceed, the power of the comb [31]. To limit the influence of the ASE, Talbot lasers usually operate below laser threshold. This is especially true in fiber configurations, where the influence of the ASE is more critical due to the confinement of the spatial mode. Whereas in free space configurations (dye or solid-state lasers), Talbot laser can produce tens of mW [37], the output power in fiber Talbot lasers usually does not exceed a fraction of mW. Recently, to operate a Talbot fiber laser above the laser threshold, we implemented an RF feedback loop, that modulates the losses of the fiber loop at the repetition rate of the pulse train [38]. This configuration brings also a solution to the deleterious influence of the ASE on the laser output, since it provides an efficient filtering of the ASE, as compared to the coherent regime. We have successfully demonstrated the generation of GHz-rate pulse trains, with an average power exceeding 1.5 mW at 4.9 GHz. At this repetition rate, the timing jitter (integrated from 10 kHz and 100 MHz) could reach 54 fs. Interestingly, we have also observed in this configuration that the phase noise at large offset frequencies from the carrier, is independent of the repetition rate. This tends to prove that some of the conclusions of the present article should also be verified in hybrid configurations, where the FSL is combined to a RF feedback loop.

We acknowledge support from the Agence Nationale de la Recherche and Direction Générale de l'Armement (Grant ANR 16-ASTR-015), and from the Association Nationale Recherche Technologie (ANRT). We also acknowledge Guillaume Arpison (TRT) for useful discussions, and for the help with the delayed self-heterodyne interferometer.

REFERENCES

[1] R. H. Walden, "Analog-to-Digital Conversion in the Early Twenty-First Century", Wiley Encyclopedia of Computer Science and Engineering, American Cancer Society, 1-14 (2008).
[2] C. Azeredo-Leme, "Clock Jitter Effects on Sampling: A Tutorial," in IEEE Circuits and Systems Magazine, 11, 26-37, (2011).
[3] A. Khilo, et al., "Photonic ADC: overcoming the bottleneck of electronic jitter," Opt. Express 20, 4454-4469 (2012).
[4] B. Murmann, "The Race for the Extra Decibel: A Brief Review of Current ADC Performance Trajectories," IEEE Solid-State Circuits Magazine 7, 5866 (2015).
[5] G. C. Valley, "Photonic analog-to-digital converters," Opt. Express 15, 1955-1982 (2012).
[6] N. R. Newbury and W. C. Swann, "Low-noise fiber-laser frequency combs (Invited)," J. Opt. Soc. Am. B 24, 1756-1770 (2007).
[7] J. Kim, M. J. Park, M. H. Perrott, and F. X. Kärtner, "Photonic subsampling analog-to-digital conversion of microwave signals at 40-GHz with higher than 7-ENOB resolution," Opt. Express 16, 16509-16515 (2008).
[8] A. Bartels, D. Heinecke, and S. A. Diddams, "Passively mode-locked 10 GHz femtosecond Ti:sapphire laser," Opt. Lett. 33 19051907 (2008).
[9] T. Steinmertz, et al., "Laser frequency combs for astronomical observations", Science, 321, 1335-1337 (2008).
[10] R. A. McCracken, J. M. Charsley and D. T. Reid, "A decade of astrocombs: recent advances in frequency combs for astronomy," Opt. Express 13, 15058-15078 (2017).
[11] X. Xie, and al., "Photonic microwave signals with zeptosecond-level absolute timing noise," Nat. Photon. 11, 44-47 (2017).
[12] F. Quinlan, S. Gee, S. Ozharar, and P. J. Delfyett, "Ultralow-jitter and -amplitude-noise semiconductor-based actively mode-locked laser," Opt. Lett. 31, 2870-2872 (2006).
[13] F. Quinlan, S. Ozharar, S. Gee, and P. J. Delfyett, "Harmonically mode-locked semiconductor-based lasers as high repetition rate ultralow noise pulse train and optical frequency comb sources," J. of Opt. A: Pure and Appl. Opt. 11, 103001 (2009).
[14] F. Rana, H. L. T. Lee, R. J. Ram, M. E. Grein, L. A. Jiang, E. P. Ippen, and H. A. Haus, "Characterization of the noise and correlations in harmonically mode-locked lasers," J. Opt. Soc. Am. B 19, 2609-2621 (2002).
[15] I. Ozdur, et al. "A Semiconductor-Based 10-GHz Optical Comb Source With Sub 3-fs Shot-Noise-Limited Timing Jitter and 500-Hz Comb Linewidth", IEEE Photon. Technol. Lett. 22, 431-433 (2010).
[16] M. V. Berry and S. Klein, "Integer, fractional and fractal Talbot effects," J. of Modern Opt. 43, 2139-2164 (1996).
[17] J. Azaña and M. A. Muriel, "Temporal Talbot effect in fiber gratings and its applications," Appl. Opt. 38, 6700-6704 (1999).
[18] D. Pudo and L. R. Chen, "Tunable Passive All-Optical Pulse Repetition Rate Multiplier Using Fiber Bragg Gratings," J. Lightwave Technol. 23, 1729 (2005).
[19] C. R. Fernandez-Pousa, F. Mateos, L. Chantada, M.-T. Flores-Arias, C. Bao, M.- V. Pérez and C. Gómez-Reino, "Timing jitter smoothing by Talbot effect. I. Variance," J. Opt. Soc. Am. B 21, 1170-1177 (2005).
[20] C. R. Fernandez-Pousa, F. Mateos, L. Chantada, M.-T. Flores-Arias, C. Bao, M.-V. Pérez and C. Gomez-Reino, "Timing jitter smoothing by Talbot effect. II. Intensity spectrum," J. Opt. Soc. Am. B 22, 753-763 (2005).
[21] D. Pudo and L. R. Chen, "Simple estimation of pulse amplitude noise and timing jitter evolution through the temporal Talbot effect," Opt. Express 15, 6351-6357 (2007).
[22] D. Pudo, C. R. Fernandez-Pousa, and L. R. Chen, "Timing Jitter Transfer Function in the Temporal Talbot Effect," IEEE Photon. Technol. Lett., 20, 496-498 (2008).
[23] L. Chantada, C. R. Fernández-Pousa, M. T. Flores-Arias, and C. Gómez-Reino, "Radio-frequency spectrum analysis of a jittery train after a second-order dispersive Talbot line," Appl. Opt. 47, E19-E26 (2008).
[24] A. Malacarne, and J. Azaña, "Analysis of amplitude fluctuation and timing jitter performance of spectrally periodic Talbot filters for optical pulse rate multiplication," Opt. Express 19, 15339-15347 (2011).

[25] J. H. Lee, Y. M. Chang, Y.-G. Han, S. H. Kim, and S. B. Lee, "2 5 times tunable repetition-rate multiplication of a 10 GHz pulse source using a linearly tunable, chirped fiber Bragg grating," Opt. Express 12, 3900-3905 (2004).
[26] R. Maram, L. Romero Cortés and J. Azaña, "Programmable Fiber-Optics Pulse Repetition-Rate Multiplier," J. of Lightwave Technol. 34, 448-455 (2016).
[27] H. Guillet de Chatellus, E. Lacot, W. Glastre, O. Jacquin, and O. Hugon, "Theory of Talbot lasers," Phys. Rev. A 88, 033828 (2013).
[28] H. Guillet de Chatellus, O. Jacquin, O. Hugon, W. Glastre, E. Lacot, and J. Marklof, "Generation of ultrahigh and tunable repetition rates in CW injection-seeded frequency-shifted feedback lasers," Opt. Express 21, 15065-15074 (2013).
[29] V. Duran, C. Schnébelin, and H. Guillet de Chatellus, "Coherent multi-heterodyne spectroscopy using acousto-optic frequency combs," Opt. Express 26, 13800-13809 (2018).
[30] H. Guillet de Chatellus, L. Romero Cortés, and J. Azaña, "Arbitrary energy-preserving control of the line spacing of an optical frequency comb over six orders of magnitude through self-imaging," Opt. Express 26, 21069-21085 (2018).
[31] N. Kanagaraj, L. Djevarhidjian, V. Duran, C. Schnébelin and H. Guillet de Chatellus, "Optimization of acousto-optic optical frequency combs," Opt. Express 27, 14842-14852 (2019).
[32] B. Schiek I. Rolfes H.J. Siweris, "Noise in HighFrequency Circuits and Oscillators", Ch.3 Measurement of Noise Parameters, John Wiley & Sons, Ltd, 73-125 (2005).
[33] E. Rochat and R. Dandliker, "New investigations on the effect of fiber amplifier phase noise," IEEE J. of Selected Topics in Quantum Electron. 7, 49-54 (2001).
[34] D. von der Linde, "Characterization of the noise in continuously operating mode-locked lasers," Appl. Phys. B 39, 201-217 (1986).
[35] H. Guillet de Chatellus, and J.-P. Pique, "Statistical properties of frequency shifted feedback lasers," Opt. Commun. 283, 71-77 (2010).
[36] L. P. Yatsenko, B. W. Shore, and K. Bergmann, "Theory of a frequency-shifted feedback laser," Opt. Commun. 236, 183-202 (2004).
[37] H. Guillet de Chatellus, O. Jacquin, O. Hugon, and E. Lacot, "Quiet broadband light," Phys. Rev. A 90, 033810 (2014).
[38] V. Billault, V. Crozatier, G. Baili, G. Feugnet, M. Schwarz, P. Nouchi, D. Dolfi, and H. Guillet de Chatellus, "Regenerative Talbot Laser for Generating Tunable Pulse Train With a Low Phase Noise," IEEE Photon. Technol. Lett., 31, 1842-1845 (2019).